Annals of Nuclear Energy 111 (2018) 271–279

Contents lists available at ScienceDirect

Annals of Nuclear Energy

journal homepage: www.elsevier.com/locate/anucene

Flexibility of ADS for minor actinides transmutation in different two-stage PWR-ADS fuel cycle scenarios

Shengcheng Zhou, Hongchun Wu, Youqi Zheng *

School of Nuclear Science and Technology, Xi'an Jiaotong University, Xi'an, Shaanxi Province 710049, China

ARTICLE INFO

Article history:
Received 14 January 2017
Received in revised form 10 July 2017
Accepted 16 August 2017
Available online 28 September 2017

Keywords:
Accelerator Driven System
Minor actinide transmutation
Pyro-chemical reprocessing
Flexibility analyses

ABSTRACT

A two-stage Pressurized Water Reactor (PWR)-Accelerator Driven System (ADS) fuel cycle is proposed as an option to transmute minor actinides (MAs) recovered from the spent PWR fuels in the ADS system. At the second stage, the spent fuels discharged from ADS are reprocessed by the pyro-chemical process and the recovered actinides are mixed with the top-up MAs recovered from the spent PWR fuels to fabricate the new fuels used in ADS. In order to lower the amount of nuclear wastes sent to the geological repository, an optimized scattered reloading scheme for ADS is proposed to maximize the discharge burnup and lower the burnup reactivity loss. Then the flexibility of ADS for MA transmutation is evaluated in this research. Three aspects are discussed, including: different cooling time of spent ADS fuels before reprocessing, different reprocessing loss of spent ADS fuels, and different top-up MAs recovered from different kinds of spent PWR fuels. The ADS system is flexible to be combined with various pyro-chemical reprocessing technologies with specific spent fuels cooling time and unique reprocessing loss. The reduction magnitudes of the long-term decay heat and radiotoxicity of MAs by transmutation depend on the reprocessing loss. The ADS system is flexible to transmute MAs recovered from different kinds of spent PWR fuels, regardless of UOX or MOX fuels. The reduction magnitudes of the long-term decay heat and radiotoxicity of different MAs by transmutation stay on the same order.

1. Introduction

The closed nuclear fuel cycle strategy and the utilization of the recycled plutonium in light water reactors (LWRs) have been determined by the Chinese government as the development roadmap of nuclear power industry in China. Until December 2015, there have been overall 28 pressurized water reactors (PWRs) in operation and 24 PWRs under construction in China (IAEA, 2016). The rapid development of nuclear power in China leads to the fast accumulation of high-level radioactive nuclear wastes (HLWs), especially minor actinides (MAs). The long-term radiotoxicity of the HLWs sent to the geological repository can be reduced by a factor of 100 if the MAs are fully recycled and incinerated (Salvatores and Palmiotti, 2011). For the incineration of MAs, the Accelerator Driven subcritical Systems (ADSs) show better safety characteristics due to the operation in subcritical state, and allow flexible fuel loading options in the core (Stanculescu, 2013; Taczanowski, 2000; Wallenius and Eriksson, 2005).

In order to lower the amount and radiotoxicity of nuclear wastes sent to the geological repository, a two-stage PWR-ADS fuel cycle is proposed as an option to transmute the minor actinides (MAs) recovered from the spent PWR fuels, as shown in Fig. 1. At the first stage, two basic fuel cycle scenarios are considered for PWR, i.e. the full utilization of uranium oxide (UOX) fuels, and the partial utilization of UOX and mixed oxide (MOX) fuels. The spent fuels discharged from the PWR core are reprocessed with the extended PUREX process to extract uranium (U), plutonium (Pu) and MAs, separately. For the UOX fuel utilization case, the recovered U and Pu are stored as the potential fuel material to be employed in the fast reactors, and the recovered MAs are incinerated in the ADS system. For the UOX/MOX fuel utilization case, the recovered U and Pu are fabricated as the MOX fuel assembly and loaded into the PWR core, and the recovered MAs are transmuted in the ADS system. At the second stage, the spent fuels discharged from ADS are reprocessed with the pyro-chemical process and the recovered actinides are mixed with the top-up MAs recovered from the spent PWR fuels to fabricate new fuels used in the ADS. In order to reduce the amount of HLWs lost to the geological repository, the discharge burnup of spent ADS fuels should be maximized and the fractional loss in the pyro-chemical process should be minimized (Yang and Khalil, 2001) (Fig. 2).

* Corresponding author at: School of Nuclear Science and Technology, Xi'an Jiaotong University, No. 28, Xianning West Road, Xi'an, Shaanxi Province, China.
E-mail address: yqzheng@mail.xjtu.edu.cn (Y. Zheng).

http://dx.doi.org/10.1016/j.anucene.2017.08.037
0306-4549/

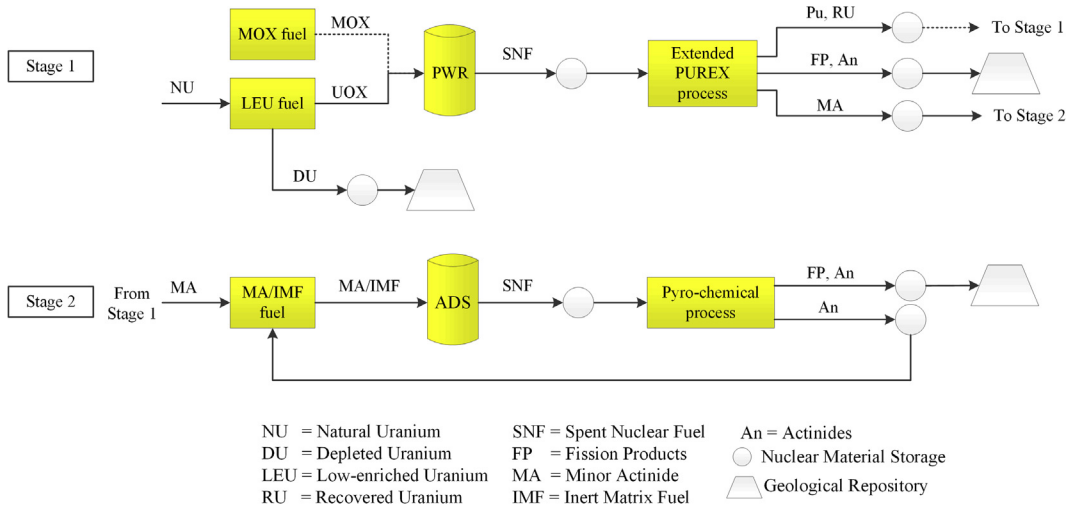

Fig. 1. Mass flow diagram of two-stage PWR-ADS fuel cycle.

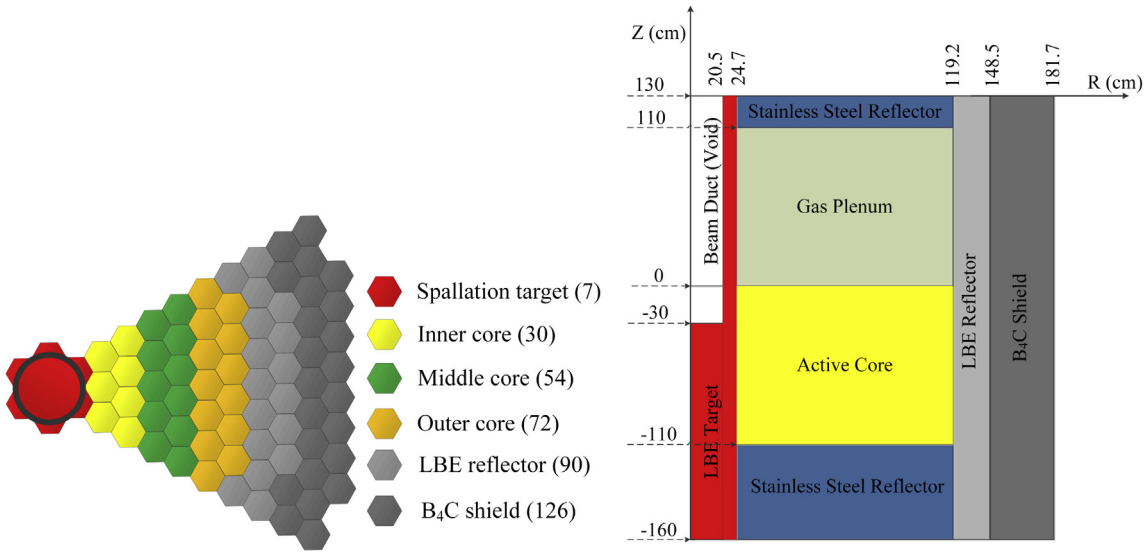

Fig. 2. Core layout of 800MWth accelerator driven minor actinide burner HEIT.

Lots of efforts have been devoted to the study of different fuel cycle scenarios using ADS to transmute transuranics (TRUs) or MAs. Cometto et al. assessed and compared the fuel cycle scenarios which employ ADS to burn TRUs recovered from the spent LWR fuels or MAs recovered from the spent LWR and fast reactor (FR) fuels (Cometto et al., 2004), and concluded that ADS is suited better as the MA burner due to the operational, technological and economic penalties. Ålander et al. simulated the fuel cycle scenarios burning TRUs recovered from spent LWR UOX or MOX fuels in ADS using the Nuclear Fuel Cycle Simulation (NFCSim) code (Ålander et al., 2006). Yang et al. evaluated the performance characteristics of a two-stage fuel cycle option involving continuous recycle of Pu in PWRs and burning of MAs in ADS (Yang et al., 2013). Most previous studies focused on the comparative study of different fuel cycle scenarios based on simplified R-Z geometry model or point depletion model, or the evaluation study of single fuel cycle scenario based on 3D neutronics calculation model. From the economic point of view, the amount of ADS in the nuclear park should be minimized and the same ADS system may be required to transmute MAs from different kinds of spent PWR fuels.

Extensive research is also carried out to develop the pyro-chemical processes to separate the actinides from the lanthanides. The pyro-chemical reprocessing process was applied for the first time as an integral part of the system in the Integral Fast Reactor (IFR) (Laidler et al., 1997). In the demonstration experiments using the nuclear fuels irradiated in the PHENIX reactor in France, 99.9% recovery of actinides was achieved with the pyro-chemical process (Malmbeck et al., 2011). However, the pyro-chemical reprocessing technology is far from maturation in the industrial scale. There are still large uncertainties on the cooling time of spent fuels before reprocessing and the reprocessing loss of actinides in the pyro-chemical process.

In this research, based on the 3D neutronics calculation model, a scattered reloading scheme for an industrial-scale accelerator driven MA burner HEIT proposed in the previous studies (Li et al., 2015) is optimized to maximize the discharge burnup and lower the burnup reactivity loss. Then the flexibility of the proposed ADS system for MA transmutation is analyzed. Three aspects are discussed, containing: different cooling time of spent ADS fuels before the pyro-chemical reprocessing, different reprocessing loss

of spent ADS fuels, and different top-up MAs recovered from different kinds of spent PWR fuels.

The remained paper is structured as follows. Section 2 introduces the design parameters of ADS and the computational methods. Section 3 describes the optimized scattered reloading scheme for ADS to maximize the discharge burnup. And Section 4 shows the flexibility of ADS for the transmutation of MAs. Finally, main conclusions are drawn in Section 5.

2. Computational model and methods

The uranium-free metallic dispersion fuel (TRU-10Zr)-Zr with pellet density of 95%TD (theoretical density) and smear density of 85%TD is adopted to sustain high burnup for MA transmutation. Here, TRU-10Zr fuel particles are dispersed in the zirconium metal matrix. The maximum achievable discharge burnup is expected to be 30 ao.% for this kind of dispersion fuel (Park et al., 2003). MA and Pu used to fabricate the dispersion fuel are recovered from the spent PWR UOX fuels with the discharge burnup of 33 GWd/tHM. The HT-9 stainless steel alloy is used as the cladding and structure materials considering its good mechanism and irradiation performance.

The subcritical core consists of the LBE target and 156 fuel assemblies surrounded by LBE reflector and B_4C shield. The active core height is 110 cm and the equivalent diameter of active core is 238.4 cm. Three enrichment zones with different inert matrix ratios in the dispersion fuel are set to flatten the radial power distribution of the subcritical core. Each fuel assembly has 271 fuel pins, and the P/D is set as 1.61. The design parameters of fuel assemblies are shown in Table 1. The coolant inlet and outlet temperatures are 300 °C and 450 °C, respectively. The effective multiplication factor k_{eff} at the beginning of the equilibrium cycle (BOEC) is 0.97 to obtain the balance of neutron economy and critical safety (Kim et al., 2002). Main performance parameters of the ADS start-up core are shown in Table 2.

The flexibility of the proposed ADS for MA transmutation is analyzed based on the equilibrium cycle. The equilibrium cycle is calculated using the core analysis code for ADS named LAVENDER (Zhou et al., 2014) in conjunction with the Monte Carlo particle transport codes FLUKA (Böhlen et al., 2014) and OpenMC (Romano et al., 2015). The spallation neutron source below 20 MeV in the target is generated using the FLUKA code, which simulates the spallation, evaporation and fission reactions in the high-energy range and the slowing down process of spallation neutrons. The region-dependent homogenized 25-group cross sections used in the neutronics analyses are generated using the OpenMC code based on the ACE format cross section library from ENDF/B-VII.1. The in-core neutron transport calculation is performed using the 3D discrete ordinate nodal transport code DNTR based on the arbitrary triangular-z meshes (Lu and Wu, 2007). The depletion calculation is performed using the Chebyshev Rational Approximation Method (CRAM), which considers 91 actinides and 1137 fission products for the transmutation analyses. Based on the equilibrium cycle search method employed in the REBUS code (Toppel, 1983), a new equilibrium cycle search procedure has been developed and implemented in LAVENDER, which can simulate the in-reactor depletion, shutdown and refueling, and the external fuel reprocessing and refabrication. In the equilibrium cycle search procedure in LAVENDER, the cycle length can be adjusted automatically to achieve the specified discharge burnup, and the fresh fuel enrichment can be searched to obtain the specified multiplication factor at any specified time during the depletion cycle.

Table 1
Design parameters of fuel assemblies.

Item	Specification
Fuel composition form	(TRU-10Zr)-Zr
Cladding material	HT-9
Bond material	Pb
Assembly pitch	177.8 mm
Number of fuel pins per assembly	271
Fuel pin diameter	6.60 mm
Pitch/diameter ratio	1.61
Cladding thickness	0.50 mm
Fuel smeared density	85%TD
Active fuel height	110.0 cm
Gas plenum height	110.0 cm

Table 2
Main performance parameters of the HEIT start-up core.

Item	Specification
Reactor power	800 MWth
Cycle length	600 EFPD
Core diameter	363.4 cm
Active core diameter	238.4 cm
Active core height	110.00 cm
Total heavy inventory	4480 kg
k_{eff}	
Initial	0.96995
Maximum	0.96995
Minimum	0.94857
Burnup reactivity swing	2.1% Δk
Coolant flow velocity	1.88 m/s
Coolant temperature (in/out)	300/450 °C
Accelerator type	proton linac
Beam energy	1.5 GeV
Beam current (max. /min.)	19. 0/ 11.4 mA
Peak linear power density (BOC/EOC)	280/306 W/cm

The equilibrium cycle performance of ADS is optimized firstly in the following section. The objective discharge burnup of the spent ADS fuels is set to 20 ao.% conservatively. The maximum allowed proton beam current provided by LINAC is 20 mA, and the peak fast fluence limit in the core is set to be 4.0×10^{23} n/cm^2 based on the irradiation experiments for the low-swelling HT-9 stainless steel alloy (Yang and Khalil, 2001).

3. Reloading scheme optimization

To achieve the targeted discharge burnup of the spent ADS fuels and lower the burnup reactivity loss, a scattered reloading scheme for ADS is optimized by varying the depletion cycle number and the cycle length.

The burnup reactivity loss over a depletion cycle $\delta\rho_c$ can be considered as the product of the average reactivity loss rate and the cycle length T_c. Similarly, discharge burnup B_d can be expressed as the product of the specific power P_s and the total fuel irradiation time nT_c, where n is the number of cycles for one batch of fuel assemblies staying in the core. The reactivity loss for one cycle $\delta\rho_c$ is assumed to be proportional to the cycle burnup B_c,

$$\delta\rho_c \propto B_c = B_d/n = P_s T_c \quad (1)$$

To lower the burnup reactivity loss $\delta\rho_c$ and achieve the targeted discharge burnup B_d, different scattered reloading schemes are proposed and compared as in Fig. 3.

For example, the repeated discharge sequences adopted in the 6.6 batch scattered reloading scheme can be expressed as follows:

Inner Core: 1–1, 1–2, 1–3, 1–4, 1–5, 1–1, ...
Middle Core: 2–1, 2–2, 2–3, 2–4, 2–5, 2–6, 2–7, 2–1, ...
Outer Core: 3–1, 3–2, 3–3, 3–4, 3–5, 3–6, 3–7, 3–1, ...

Here the couple of digits (x-y) is named as the discharge/reloading index. The first digit x means the index of the fuel management

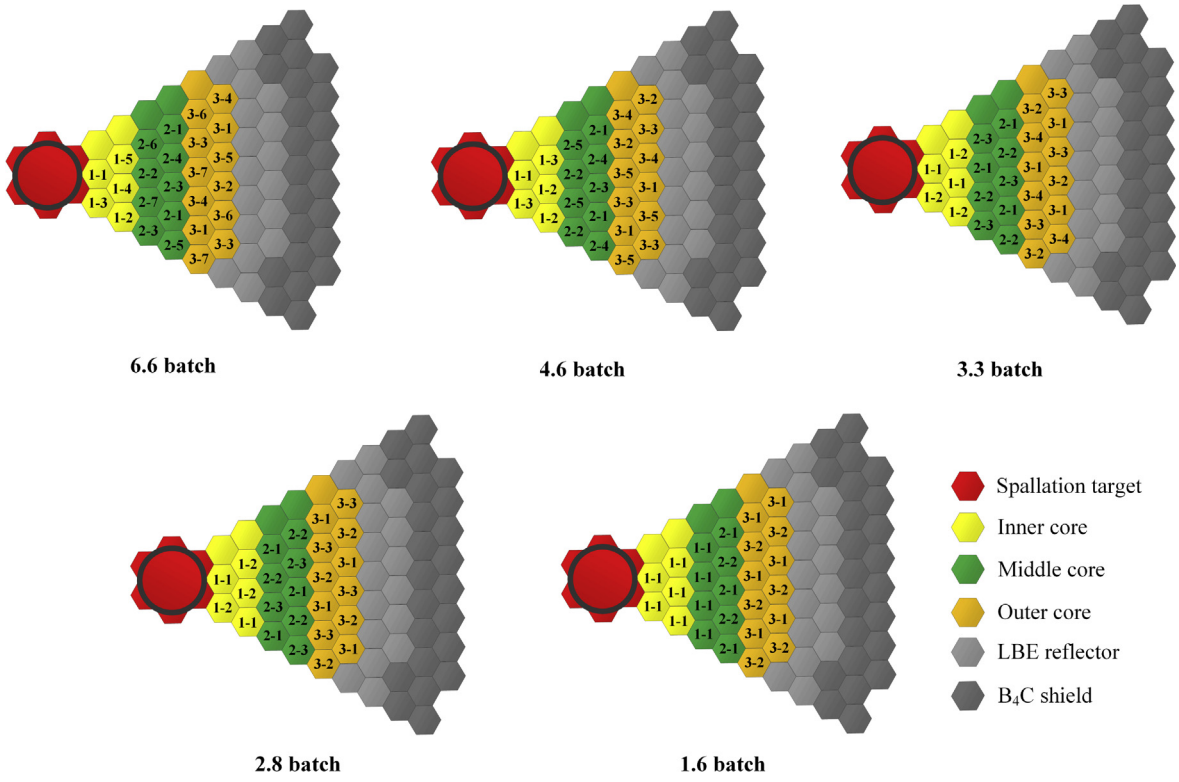

Fig. 3. Multi-batch scattered reloading schemes.

path, and the second digit y means the discharge/reloading sequence number in the specified fuel management path. The fuel management path describes a list of discharge/reloading operations for a cluster of fuel assemblies, which may be located in different regions. The fuel assemblies with the same discharge/reloading index are discharged from the ADS at the same time. The refueling batch number of the fuel assemblies located in the inner core is reduced to meet the fast fluence limit of the regions near the spallation target. In the 1.6 batch reloading scheme, the refueling batch number of the fuel assemblies located in the inner ring of the middle core is also reduced to single batch to lower the local fast fluence accumulation. To simply the reloading scheme specification, the fuel management operations of the single batch refuelled fuel assemblies in the inner core and the inner ring of the middle core are specified in a merged way as one fuel management path. So the first digit of the discharge/reloading index is denoted as "1" for the fuel assemblies in the inner ring of the middle core.

The equilibrium cycle performance of each scattered reloading scheme is calculated using the LAVENDER code, and the in-core neutron transport calculation is performed with S_6 discrete ordinates for the 1/6 core. Fig. 4 shows the proton beam current at the end of the equilibrium cycle (EOEC) and the burnup reactivity loss for different refueling batch numbers. The burnup reactivity loss and proton beam current at EOEC decrease monotonically with the increased refueling batch number, and almost converge when the refueling batch number reaches 6.6. When the refueling batch number is smaller than 2, the proton beam current at EOEC exceeds the maximum allowed proton beam current 20 mA. Fig. 5 shows the peak fast fluence and the cycle length for each scattered reloading scheme. The peak fast fluence also exceeds the design limit 4.0×10^{23} n/cm^2 when the refueling batch number is smaller than 2. The cycle length decreases monotonically with the increased refueling batch number, which means more frequent

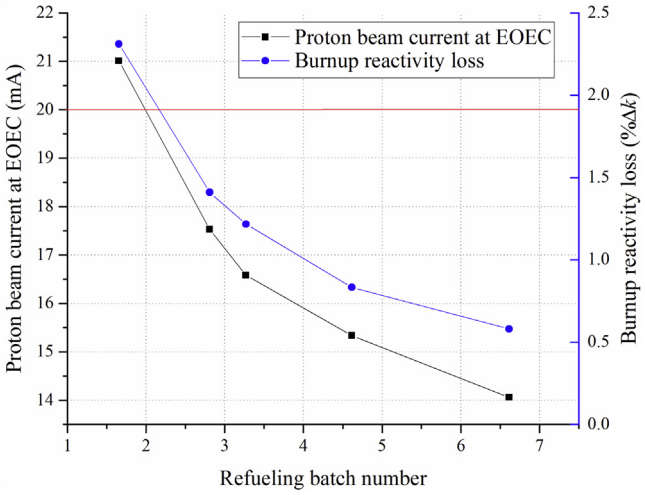

Fig. 4. Proton beam current and burnup reactivity loss as functions of refueling batch number.

refueling operations are required. However, more frequent refueling may not adversely impact the load factor, since the ADS system requires periodic shutting down for maintenance or replacement of accelerator, beam delivery and spallation target components (Yang et al., 2013).

Based on above analyses, the refueling batch number should be larger than 2 to satisfy the design constraints of the proton beam current and peak fast fluence in the core. The 6.6 batch scattered reloading scheme is finally selected due to the low burnup reactivity loss (0.56%Δk) and relaxed requirement for the proton beam current at EOEC (14.0 mA).

4. Flexibility of ADS for MA transmutation

4.1. Cooling time of spent ADS fuels before reprocessing

Three cases are compared to evaluate the flexibility of ADS in conjunction with the pyro-chemical processes with different spent fuel cooling time before reprocessing, which are 200 days, 600 days and 1200 days, respectively. The performance parameters of ADS are shown in Table 3. With the increase of cooling time, more reactive nuclides, such as ^{238}Pu and ^{241}Pu, decay into less reactive nuclides, which reduces the reactivity of the recycled actinides. Therefore, larger heavy metal (HM) inventory is required to achieve the targeted multiplication factor at BOEC. The heavy metal inventory at BOEC is almost proportional to the cooling time, and about 200 kg heavy metal inventory is required additionally if the cooling time increases by 1000 days. Longer cycle length is necessary to obtain the same targeted discharge burnup for the ADS with larger heavy metal inventory.

However, the peak fast fluence in the core is quite close to the design limit if 200 days cooling is adopted. To meet the design constraints, there must be some penalty of the discharge burnup. When the cooling time increases from 200 days to 1200 days, about 2.8% penalty of the discharge burnup is afforded by shortening the cycle length.

The transmutation performance is evaluated by the comparison of the radiotoxicity and decay heat of the top-up MAs fed into the ADS and those of the lost fission products (FPs) and actinides (An) which are sent to the geological repository. The dose coefficients for calculating the radiotoxicity come from the ICRP official report (Eckerman et al., 2013). Fig. 6 shows the decay heat of the top-up MAs and the lost FPs and An for different cooling time. The reduction magnitude of the decay heat of top-up MAs by transmutation in ADS is quite close after 10 years for different cooling time. Fig. 7

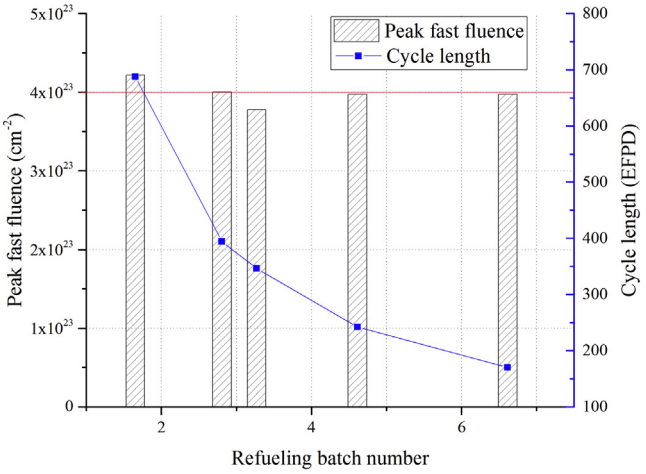

Fig. 5. Peak fast fluence and cycle length variations with refueling batch number.

Table 3
Performance characteristics of the equilibrium ADS for different cooling time.

Case	1	2	3
Spent fuel cooling time (day)	200	600	1200
Thermal power (MW)	800	800	800
Cycle length (EFPD)	170.1	173.4	172.4
Heavy metal inventory (kg)			
BOEC	4291.9	4374.2	4487.0
EOEC	4151.0	4230.6	4344.1
Fuel particle fraction (vol%) (Inner/Middle/Outer)	15.6/21.9/ 28.2	15.95/ 22.33/28.71	16.32/ 22.85/29.37
k_{eff} (BOEC/EOEC)	0.9701/ 0.9643	0.9701/ 0.9647	0.9701/ 0.9654
Burnup reactivity loss (%Δk)	0.575	0.543	0.472
k_s (BOEC/EOEC)	0.9567/ 0.9493	0.9566/ 0.9497	0.9564/ 0.9505
Beam current (mA)(BOEC/EOEC)	11.90/ 14.01	11.89/13.87	11.93/13.62
Average power density (W·cm^{-3})	170.2	170.2	170.2
3D Powe peaking factor			
BOEC	1.555	1.554	1.564
EOEC	1.639	1.637	1.635
Peak power density (W·cm^{-3})			
BOEC	264.7	264.6	266.2
EOEC	279.0	278.7	278.4
Average discharge burnup (ao.%)	19.86	19.87	19.31
Peak fast fluence (10^{23} cm^{-2})	3.941	3.996	3.948
Net HM consuming rate (kg·EFPY^{-1})	302.7	302.8	302.9
Equilibrium loading (kg·EFPY^{-1})			
Top-up MA	303.9	304.0	304.2
Recycled HM	1209.4	1208.6	1251.9
Total HM	1513.3	1512.6	1556.1

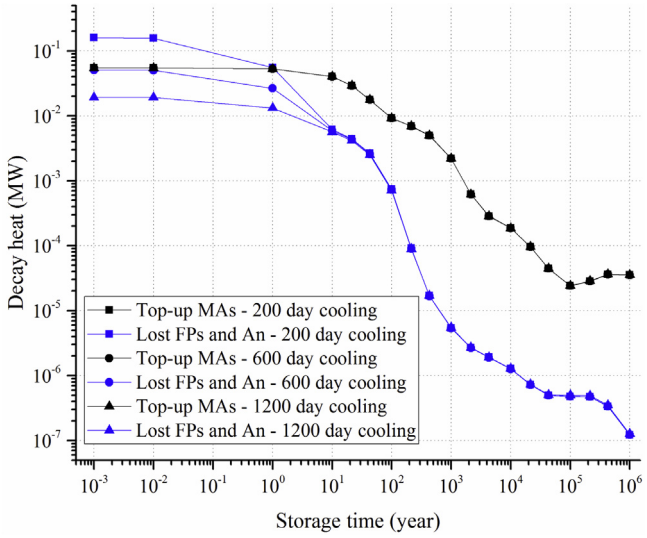

Fig. 6. Decay heat of top-up MAs and lost FPs and An for different cooling time.

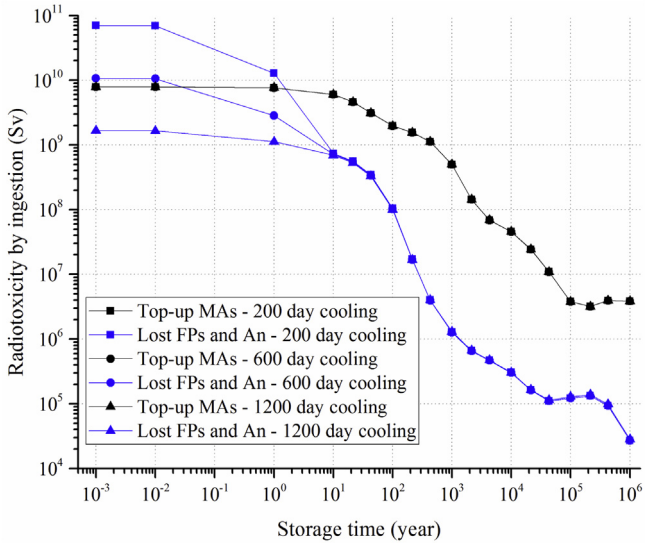

Fig. 7. Radiotoxicity of top-up MAs and lost FPs and An for different cooling time.

Table 4
Performance characteristics of the equilibrium ADS for different reprocessing loss.

Case	1	2	3	4
Reprocessing loss	0.0%	0.1%	0.2%	0.5%
Thermal power (MW)	800	800	800	800
Cycle length (EFPD)	169.9	170.1	170.3	170.9
Heavy metal inventory (kg)				
BOEC	4287.4	4291.9	4296.2	4310.0
EOEC	4146.6	4151.0	4155.1	4168.4
Fuel particle fraction (vol%) (Inner/Middle/Outer)	15.6/21.9/28.1	15.6/21.9/28.2	15.7/21.9/28.2	15.7/22.0/28.3
k_{eff} (BOEC/EOEC)	0.9700/0.9642	0.9701/0.9643	0.9701/0.9643	0.9701/0.9646
Burnup reactivity loss (%Δk)	0.582	0.575	0.571	0.552
k_s (BOEC/EOEC)	0.9568/0.9493	0.9567/0.9493	0.9566/0.9494	0.9566/0.9496
Beam current (mA) (BOEC/EOEC)	11.87/14.03	11.90/14.01	11.93/14.00	11.92/13.92
Average power density (W·cm^{-3})	170.2	170.2	170.2	170.2
3D Powe peaking factor				
BOEC	1.554	1.555	1.555	1.555
EOEC	1.639	1.639	1.638	1.635
Peak power density (W·cm^{-3})				
BOEC	264.6	264.7	264.7	264.8
EOEC	279.0	279.0	278.8	278.4
Average discharge burnup (ao.%)	19.86	19.86	19.87	19.87
Peak fast fluence (10^{23} cm^{-2})	3.938	3.941	3.943	3.952
Net HM consuming rate (kg·EFPY^{-1})	302.7	302.7	302.7	302.7
Equilibrium loading (kg·EFPY^{-1})				
Top-up MA	302.7	303.9	305.1	308.7
Recycled HM	1210.7	1209.4	1208.1	1204.1
Total HM	1513.4	1513.3	1513.2	1512.8

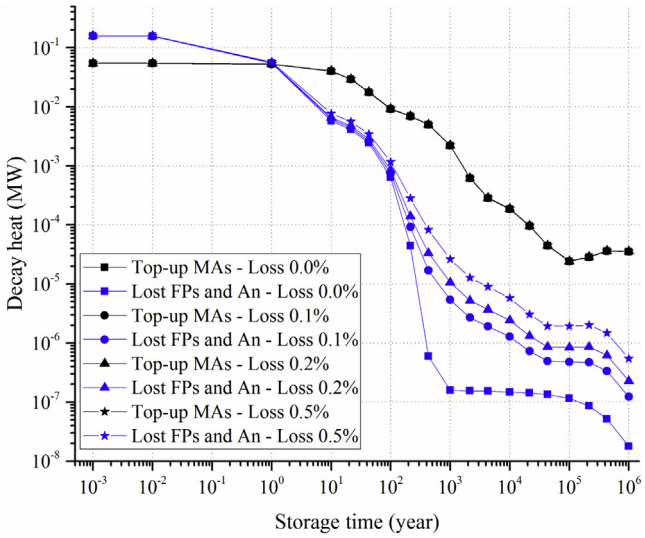

Fig. 8. Decay heat of top-up MAs and lost FPs and An for different reprocessing loss.

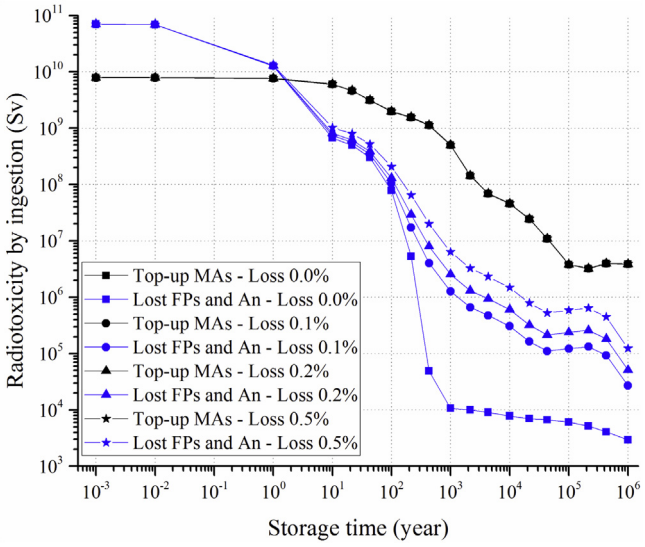

Fig. 9. Radiotoxicity of top-up MAs and lost FPs and An for different reprocessing loss.

shows the results of radiotoxicity, and similar tendency can be observed. The lost FPs and An can be cooled in the interim storage before being sent to the geological repository, and the impact of the cooling time of spent ADS fuels is neglectable in long run. Thus the ADS system is flexible with different cooling time of spent ADS fuels before reprocessing.

4.2. Reprocessing loss of spent ADS fuels

Four cases are discussed to analyze the impact of the reprocessing loss of spent ADS fuels at the second stage. The loss fractions are assumed by extending the current pyro-chemical reprocessing technologies to the industrial scale, i.e. 0.0%, 0.1%, 0.2% and 0.5% for all the actinides, and the performance parameters of ADS are shown in Table 4. The heavy metal inventory and the top-up MA mass increase slightly with the reprocessing loss to compensate the actinides lost to the geological repository, and the burnup reactivity loss and the proton beam current decrease fractionally with the rising heavy metal inventory. The influence of the reprocessing loss on the performance of ADS is reasonably small.

The decay heat and radiotoxicity of the top-up MAs and the lost FPs and An are shown in Figs. 8 and 9 for different reprocessing loss, respectively. The reduction magnitudes of the decay heat and radiotoxicity of the top-up MAs by transmutation are almost proportional to the reprocessing loss. When the reprocessing loss of the actinides is no more than 0.2%, the reduction magnitudes of the radiotoxicity and decay heat of the top-up MAs can be larger than 2 orders after 1000 years.

The ADS system is flexible to be deployed with the pyro-chemical processes with different reprocessing loss of actinides. Significant reduction of the decay heat and radiotoxicity of MAs can only be achieved by limiting the reprocessing loss of actinides below 0.2% in the pyro-chemical process at the second stage.

Table 5
Compositions of MAs recovered from different spent PWR fuels (wt%).

Case Spent PWR fuel	1 UOX 33 GWd/tHM	2 UOX 45 GWd/tHM	3 CORAIL 45 GWd/tHM	4 UOX&MOX 45 GWd/tHM
^{237}Np	56.18	49.65	12.33	3.884
^{238}Pu	0	0	0.03	0
^{239}Pu	0	0	2.52	0
^{240}Pu	0	0.32	1.72	0
^{241}Pu	0	0	0.85	0
^{242}Pu	0	0	2.05	0
^{241}Am	26.4	32.1	30.93	75.51
^{242} mAm	0	0.06	0.22	0.254
^{243}Am	12	13.37	32.29	16.054
^{242} Cm	0	0	0	0
^{243} Cm	0.03	0.03	0.08	0.066
^{244}Cm	5.11	4.04	14.86	3.001
^{245}Cm	0.28	0.39	1.95	1.139
^{246}Cm	0	0.04	0.17	0.091

Table 6
Performance characteristics of the equilibrium ADS for MAs from different spent PWR fuels.

Case Spent PWR fuel	1 UOX 33 GWd/tHM	2 UOX 45 GWd/tHM	3 CORAIL 45 GWd/tHM	4 UOX&MOX 45 GWd/tHM
Thermal power (MW)	800	800	800	800
Cycle length (EFPD)	170.1	172.4	157.8	168.5
Heavy metal inventory (kg)				
BOEC	4291.9	4345.6	4251.9	4516.3
EOEC	4151.0	4202.8	4121.0	4376.7
Fuel particle fraction (vol%) (Inner/Middle/Outer)	15.6/21.9/28.2	15.8/22.2/28.5	15.4/21.6/27.8	16.4/22.9/29.5
k_{eff} (BOEC/EOEC)	0.9701/0.9643	0.9701/0.9644	0.9697/0.9600	0.9701/0.9648
Burnup reactivity loss (%Δk)	0.575	0.571	0.965	0.530
k_s (BOEC/EOEC)	0.9567/0.9493	0.9567/0.9492	0.9579/0.9449	0.9565/0.9498
Beam current (mA) (BOEC/EOEC)	11.90/14.01	11.93/14.10	11.96/15.86	12.27/14.26
Average power density (W·cm^{-3})	170.2	170.2	170.2	170.2
3D Power peaking factor				
BOEC	1.555	1.555	1.534	1.554
EOEC	1.639	1.639	1.672	1.628
Peak power density (W·cm^{-3})				
BOEC	264.7	264.7	261.2	264.5
EOEC	279.0	279.1	284.7	277.1
Average discharge burnup (ao.%)	19.86	19.87	18.69	18.77
Peak fast fluence (10^{23} cm^{-2})	3.941	3.997	3.946	3.980
Net HM consuming rate (kg·EFPY^{-1})	302.7	302.7	303.2	303.1
Equilibrium loading (kg·mn^2 EFPY^{-1})				
Top-up MA	303.9	303.9	304.5	304.3
Recycled HM	1209.4	1208.3	1303.6	1295.2
Total HM	1513.3	1512.2	1608.1	1599.6

4.3. MAs recovered from different spent PWR fuels

This subsection investigates the flexibility of ADS for transmuting different MAs recovered from different kinds of spent PWR fuels. Four kinds of typical spent PWR fuels are considered as follows: spent PWR UOX fuels with discharge burnup of 33.0 GWd/tHM and 45.0 GWd/tHM (Sasa et al., 2001; Tsujimoto et al., 2004), spent PWR UOX and MOX fuels with discharge burnup of 45.0 GWd/tHM from the CORAIL concept PWR (Yang et al., 2013), and spent PWR UOX (90%) and MOX (10%) fuels with discharge burnup of 45.0 GWd/tHM (Artioli et al., 2008). The specific compositions of MAs are shown in Table 5. The performance parameters of ADS are shown in Table 6.

Firstly, the performance parameters of ADS for transmuting MAs recovered from different spent PWR UOX fuels are compared. For Case 1 and Case 2, sufficiently small differences of the heavy metal inventory, burnup reactivity loss and proton beam current can be found, and the peak power density and 3D power peaking factor at BOEC and EOEC are also quite close. Furthermore, the reduction magnitudes of the radiotoxicity and decay heat of MAs by transmutation are very similar, as shown in Figs. 10 and 11. It is indicated that for the spent PWR UOX fuels, discharge burnup has neglectable impact on the transmutation performance. The ADS system is flexible to transmute MAs recovered from different spent PWR UOX fuels.

Secondly, the comparisons between the cases transmuting MAs recovered from the spent UOX fuels and the mixed spent UOX/MOX fuels are performed, considering the same discharge burnup. Compared with Case 2, larger heavy metal inventory is required in Case 4 to achieve the targeted multiplication factor at BOEC. It results from that the MAs recovered from the mixed spent UOX/MOX fuels mainly consist of ^{241}Am, which is less reactive than that recovered from the spent UOX fuels. Due to the peak fast fluence limit in the core, about 5% penalty of the discharge burnup should be afforded.

As to the performance parameters of ADS transmuting MAs recovered from the CORAIL spent fuels (Case 3), the heavy metal inventory at BOEC decreases slightly. The burnup reactivity loss rises significantly by 69%, and the proton beam current at EOEC increases by 12.5%. These mainly due to that a small fraction of

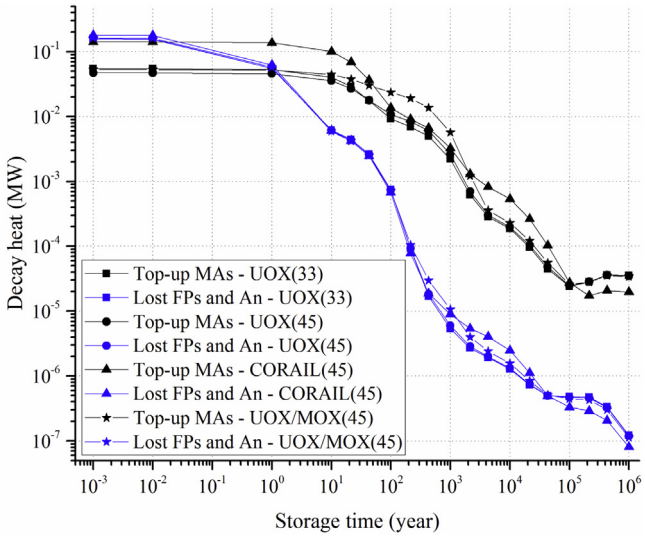

Fig. 10. Decay heat of top-up MAs and lost FPs and An for MAs from different spent PWR fuels.

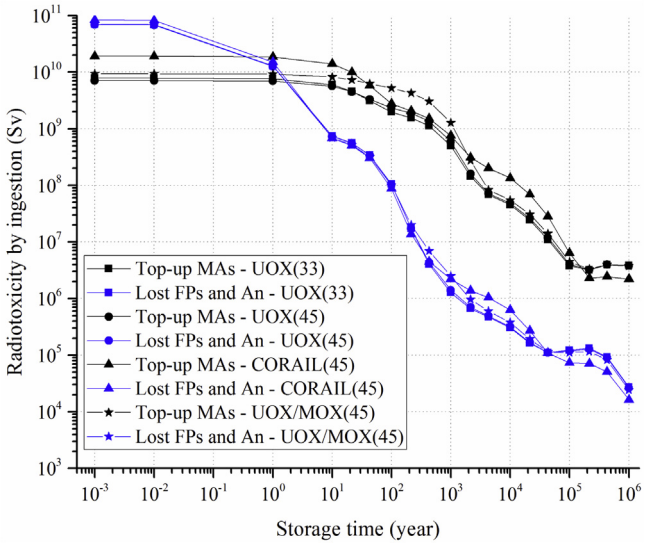

Fig. 11. Radiotoxicity of top-up MAs and lost FPs and An for MAs from different spent PWR fuels.

highly reactive Pu isotopes are mixed into the MAs in the extended PUREX process dealing with the CORAIL spent fuels. The peak power density and 3D power peaking factor at EOEC also increase because of the stronger spallation neutron source at EOEC, which results in the fast accumulation of fast fluence in the core. Thus, about 6% penalty of the discharge burnup has to be afforded by reducing the cycle length to guarantee the peak fast fluence meeting the design constraints.

Figs. 10 and 11 show the decay heat and radiotoxicity of the top-up MAs and the lost FPs and An for different spent PWR fuels, respectively. The decay heat and radiotoxicity of the top-up MAs increase slightly with the increased discharge burnup of spent UOX fuels, and increase further if the MOX fuels are utilized in PWR. Compared with the cases transmuting MAs from the spent UOX fuels (Case 1 and 2), the reduction magnitudes of the decay heat and radiotoxicity of MAs from the spent UOX/MOX fuels (Case 3 and 4) are higher, but no essential differences can be observed.

5. Conclusions

The two-stage PWR-ADS fuel cycle is analyzed in this research. In order to reduce the amount of nuclear wastes sent to the geological repository and lower the burnup reactivity loss of ADS, a series of scattered reloading schemes with different refueling batch numbers are compared. As the refueling batch number increases, the burnup reactivity loss and the proton beam current at EOEC decrease. Thus the 6.6 batch scattered reloading scheme is selected as the optimized fuel management strategy for further fuel cycle analyses.

Main conclusions drawn in the fuel cycle analyses are summarized as follows:

1) Larger heavy metal inventory is required to achieve the targeted multiplication factor at BOEC with longer cooling time of the spent ADS fuels before reprocessing. Penalty of the discharge burnup is necessary by shortening cycle length to satisfy the peak fast fluence limit. But the cooling time has little influence on the transmutation performance of ADS.
2) The reprocessing loss almost has no impacts on the performance of ADS but determines the reduction magnitudes of the decay heat and radiotoxicity of MAs by transmutation.
3) The ADS system is flexible to transmute MAs recovered from different spent PWR fuels. Some penalty of the discharge burnup needs to be afforded to meet the peak fast fluence constraints. Mixing fissile Pu isotopes into the MAs recovered from the spent PWR fuels should be avoided, which is very harmful to the reduction of the burnup reactivity loss. The reduction magnitudes of the decay heat and radiotoxicity of MAs by transmutation show no significant differences for different spent PWR fuels.

Acknowledgments

This work is supported partly by the National Natural Science Foundation of China (Approved Number: 11475134, 11522544). The first author is grateful for the valuable discussion about the equilibrium cycle search method and scattered reloading scheme with Prof. Won Sik Yang and Dr. Tongkyu Park at Purdue University.

References

Ålander, A., Dufek, J., Gudowski, W., 2006. From once-through nuclear fuel cycle to accelerator-driven transmutation. Nucl. Instrum. Methods Phys. Res., Sect. A 562, 630–633.

Artioli, C., Chen, X., Gabriellib, F., Glinatsis, G., 2008. Minor actinide transmutation in ADS: the EFIT core design. In: International Conference on the Physics of Reactors, Interlaken, Switzerland.

Böhlen, T.T., Cerutti, F., Chin, M.P.W., Fassò, A., Ferrari, A., Ortega, P.G., Mairani, A., Sala, P.R., Smirnov, G., Vlachoudis, V., 2014. The FLUKA Code: developments and challenges for high energy and medical applications. Nucl. Data Sheets 120, 211–214.

Cometto, M., Wydler, P., Chawla, R., 2004. A comparative physics study of alternative long-term strategies for closure of the nuclear fuel cycle. Ann. Nucl. Energy 31, 413–429.

Eckerman, K., Harrison, J., Menzel, H.G., Clement, C.H., 2013. ICRP Publication 119: compendium of dose coefficients based on ICRP Publication 60. Ann. ICRP 42, e1–e130.

IAEA, 2016. Nuclear Power Reactors in the World. International Atomic Energy Agency, Vienna.

Kim, Y., Park, W.S., Yang, W.S., Hill, T.A.T.R.N., 2002. An investigation of an optimal range of subcriticality for accelerator-driven systems, PHYSOR 2002, Seoul, Korea.

Laidler, J.J., Battles, J.E., Miller, W.E., Ackerman, J.P., Carls, E.L., 1997. Development of pyroprocessing technology. Prog. Nucl. Energy 31, 131–140.

Li, X., Zhou, S., Zheng, Y., Wang, K., Wu, H., 2015. Preliminary studies of a new accelerator-driven minor actinide burner in industrial scale. Nucl. Eng. Des. 292, 57–68.

Lu, H., Wu, H., 2007. A nodal SN transport method for three-dimensional triangular-z geometry. Nucl. Eng. Des. 237, 830–839.
Malmbeck, R., Nourry, C., Ougier, M., Souček, P., Glatz, J.P., Kato, T., Koyama, T., 2011. Advanced fuel cycle options. Energy Procedia 7, 93–102.
Park, W.S., Song, T.Y., Lee, B.O., Park, C.K., 2003. A preliminary design study for the HYPER system. Nucl. Eng. Des. 219, 207–223.
Romano, P.K., Horelik, N.E., Herman, B.R., Nelson, A.G., Forget, B., Smith, K., 2015. OpenMC: a state-of-the-art Monte Carlo code for research and development. Ann. Nucl. Energy 82, 90–97.
Salvatores, M., Palmiotti, G., 2011. Radioactive waste partitioning and transmutation within advanced fuel cycles: achievements and challenges. Prog. Part. Nucl. Phys. 66, 144–166.
Sasa, T., Tsujimoto, K., Takizuka, T., Takano, H., 2001. Code development for the design study of the OMEGA Program accelerator-driven transmutation systems. Nucl. Instrum. Methods Phys. Res., Sect. A 463, 495–504.
Stanculescu, A., 2013. Accelerator driven systems (ADSs) for nuclear transmutation. Ann. Nucl. Energy 62, 607–612.
Taczanowski, S., 2000. Evaluation of accelerator-driven subcritical systems for transmutations of nuclear waste. Int. J. Energy Res. 24, 935–951.
Toppel, B.J., 1983. A User's Guide for the REBUS-3 Fuel Cycle Analysis Capability. Argonne National Laboratory, USA.
Tsujimoto, K., Sasa, T., Nishihara, K., Oigawa, H., Takano, H., 2004. Neutronics design for lead-bismuth cooled accelerator-driven system for transmutation of minor actinide. J. Nucl. Sci. Technol. 41, 21–36.
Wallenius, J., Eriksson, M., 2005. Neutronics of minor-actinide burning accelerator-driven systems with ceramic fuel. Nucl. Technol. 152, 367–381.
Yang, W.S., Khalil, H.S., 2001. Blanket design studies of a lead-bismuth eutectic–cooled accelerator transmutation of waste system. Nucl. Technol. 135, 162–182.
Yang, W.S., Kim, T.K., Taiwo, T.A., 2013. Performance evaluation of two-stage fuel cycle based on PWR and ADS, ICAPP 2013, Jeju Island, Korea.
Zhou, S., Wu, H., Cao, L., Zheng, Y., Huang, K., He, M., Li, X., 2014. LAVENDER: A steady-state core analysis code for design studies of accelerator driven subcritical reactors. Nucl. Eng. Des. 278, 434–444.